Direct Detection of the Solvent Molecules between Solid Surfaces with Simultaneous Adhesion Force Measurement

Takashi Kodama,*,†,‡ Hideo Arakawa,§ Atsushi Ikai,‖ and Hiroyuki Ohtani‡

Department of Mechanical Engineering, Stanford University, Stanford, California 94305, Department of Biomolecular Engineering, Tokyo Institute of Technology, Yokohama 226-8501, Japan, Bio Nanomaterials Group, Organic Nanomaterials Center (ONC), National Institute for Materials Science (NIMS), Ibaraki 305-0044, Japan, and Department of Life Science, Tokyo Institute of Technology, Yokohama 226-8501, Japan

In this study, we applied the force curve mode confocal laser scanning/atomic force microscope (CLSM/AFM) to detect solvent properties in the contact area with the simultaneous force measurement. Two experimental approaches were carried out. First, we performed an adhesion force measurement between a carboxylated polystyrene microbead and the substrate surface that has the terminus group of $-NH_2$ or $-CF_3$ at various pH by the traditional AFM measurement. The results revealed that the hydrophobic interaction and hydrogen bonding force operates when the microbead is brought into contact with the $-CF_3$ and $-NH_2$ surface, respectively. Next, the solvent molecules between solid surfaces were detected with the simultaneous adhesion force measurement by the CLSM/AFM system. The results revealed that the fluorescence intensity of fluorescein was decreased only when the hydrophobic interaction worked. It was due to the removal of solvent molecules in the contact area, and the hydrophobic surfaces stabilize each other by making the contact area hydrophobic. On the other hand, when the hydrophilic interaction, such as hydrogen bonding, operates, the solvent molecules exist in the contact area.

1. Introduction

In the field of physics, it is important to measure the interaction between various molecules and surfaces and to reveal the basic theory underlying this interaction. There are various types of interactions between surfaces in liquids, such as the diffuse electric double layer force, hydrophobic interaction, and structural force by regulating the solvent molecules.[1] Thus, many researchers have measured the interactions between various surfaces in liquids, and a substantial number of experimental results have been reported that have used atomic force microscopy (AFM) and a surface force apparatus.[2–7] These results have revealed that the solvent property in the contact area is closely related to the surface force. Among such surface forces, the adhesion force has been studied well because it can be detected with high sensitivity.[8–24] Various adhesion force experiments have been carried out with the variation of the surface property by modification with self-assembled monolayers.[14–24] These results reveal that the adhesion force has a dependence on the surface composition and solvent property. Hydrogen bonding force, hydrophobic interaction, and electrostatic force operate mainly between the surfaces and depend on the ionization state of the functional groups. Furthermore, some applications of the adhesion force measurement have been reported. It has recently been applied to map the spatial arrangement of the chemical functional groups on a sample surface by the detection of the differences in the adhesion or frictional forces.[8–13] In addition,

the pKa measurement of the terminal groups on the surface can be carried out with great sensitivity by the adhesion force measurement with the variation of the pH. For example, it has been reported that the pK_a value of an amino group on a surface is approximately 4.0, whereas it is between 9 and 10 in a bulk solution. It has also been reported that the pK_a value of a $-COOH$ group is approximately 6.0.[16] Such large pK_a shifts occur because of (1) the presence of a low dielectric permittivity region surrounding the acidic or basic group, (2) the changes in the number of degrees of freedom of the immobilized species, and (3) the excess electrostatic free energy of the supporting surface and change in the dielectric constant of the solution in the vicinity of the charged surface.[16] These shifts have been measured with contact angle experiments.[25–28]

As mentioned above, adhesion force measurements between solid surfaces in liquids are important, and these forces are sensitive to various solvent molecules, ionic strengths, pH, and surface compositions. Therefore, it is important to discuss the relation between the adhesion force and solvent property in the contact area. Thus far, surface force measurements have been performed by varying the aqueous conditions in order to determine the relation between the solvent property and the surface forces. However, it was difficult to carry out "direct" measurements of the solvent property in the contact area with classical force measurement methods. Therefore, we proposed a "direct" method to observe the solvent property in the contact area by the simultaneous adhesion force measurement using a force curve mode confocal laser scanning microscope (CLSM)/ AFM system (see Figure 1).[29–32] This enables us to measure the fluorescence spectra in the contact area with a simultaneous force curve measurement. If the solvent property in the contact area can be determined simultaneously, this method will become a powerful technique for revealing the fundamental physics
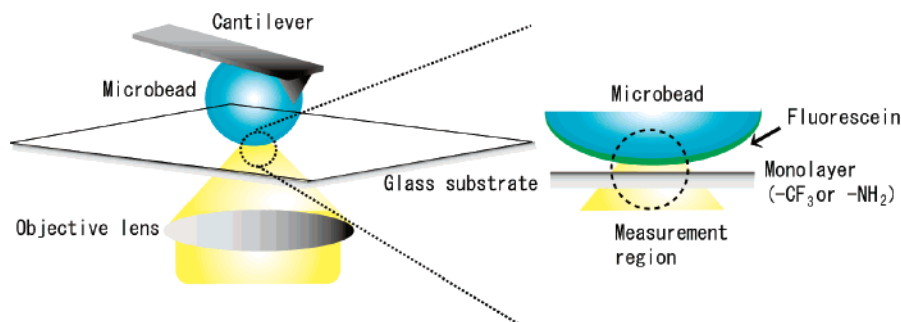
　* Author to whom correspondence should be addressed. E-mail: tkodama@ bio.titech.ac.jp.
　† Stanford University.
　‡ Department of Biomolecular Engineering, Tokyo Institute of Technology.
　§ NIMS.
　‖ Department of Life Science, Tokyo Institute of Technology.

Direct Detection of the Solvent Molecules

J. Phys. Chem. C, Vol. 111, No. 19, 2007 **7099**

Figure 1. Schematic diagram of the force curve measurement mode for the CLSM/AFM system. The force curve measurement was performed with a simultaneous measurement of the solvent property in the contact area of an AFM probe when a microbead was attached to the end of the probe.

involved. Furthermore, the spectroscopic data can be provided as additional information to the standard AFM measurement data. Thus, this technique can be applied to various AFM measurements.

In this study, as an initial trial, we applied the force curve mode CLSM/AFM technique to observe the water molecules between a polystyrene microbead, which is attached to the end of an AFM tip, and hydrophilic or hydrophobic surfaces. Fluorescein-5-maleimide (FLU) was used as the fluorescent probe for the detection of the solvent properties. FLU is a pH-sensitive fluorophore, and its chemical structures are shown in Figure 2a. Furthermore, the pH-dependence of the absorption and fluorescence spectra is shown in Figure 2, panels b and c, respectively. FLU has two types of ionizable groups: $-COOH$ and aromatic $-OH$. The pK_a's of these groups are approximately 3 and 7, respectively. It is well-known that FLU is more fluorescent in the H^+-dissociated form than in the H^+-undissociated form. Therefore, it cannot emit intense fluorescence when it is in the hydrophobic condition. By applying this optical property, FLU was introduced onto the surface of an AFM probe, and the fluorescence intensity change was measured when the AFM probe was brought into contact with the hydrophilic or hydrophobic surfaces.

2. Materials and Methods

2.1. Preparation of the Sample. A carboxylated polystyrene microbead (Polybead Carboxylate Microspheres, $r = 5$ μm, Polysciences, Warrington, PA) was attached to the end of an AFM cantilever (NP$-$S, spring constant = 0.12 N/m, Digital Instruments, Santa Barbara, CA) using micro manipulators (MMN-1, MMO-202ND, and MN-153, Narisige, Japan) to increase the number of dye molecules in the contact area[29$-$35] for better spectroscopic measurement. FLU (FLU, Molecular probes, Eugene, OR) was used as the fluorescent probe in identifying the solvent properties. It was covalently cross-linked to the carboxylated surface of the microbead, as described below. After the attachment of the microbead to the AFM cantilever, the condensation of the carboxyl group of the bead and *N*-hydroxysulfosuccinimide (Sulfo-NHS, Pierce, Rockford, IL) with 1-[3-(dimethylamino)propyl]-3-ethylcarbodiimide hydrochloride (EDC, Pierce, Rockford, IL) produced an active intermediate,[33] which upon reaction with a cysteine formed an $-SH$ terminated residue. The $-SH$ group was used for the introduction of FLU.

Cover glass was used as the substrate after the modification with 3-(diethoxymethylsilyl)propylamine (APDS) or dimethoxymethyl(3,3,3-trifluoropropyl)silane (FPDS) (Sigma, St. Louis, MO) by the silane coupling method.[36,37]

2.2. Experimental Equipment. Figure 1 shows a schematic diagram of the measurement system.[30] This system is composed
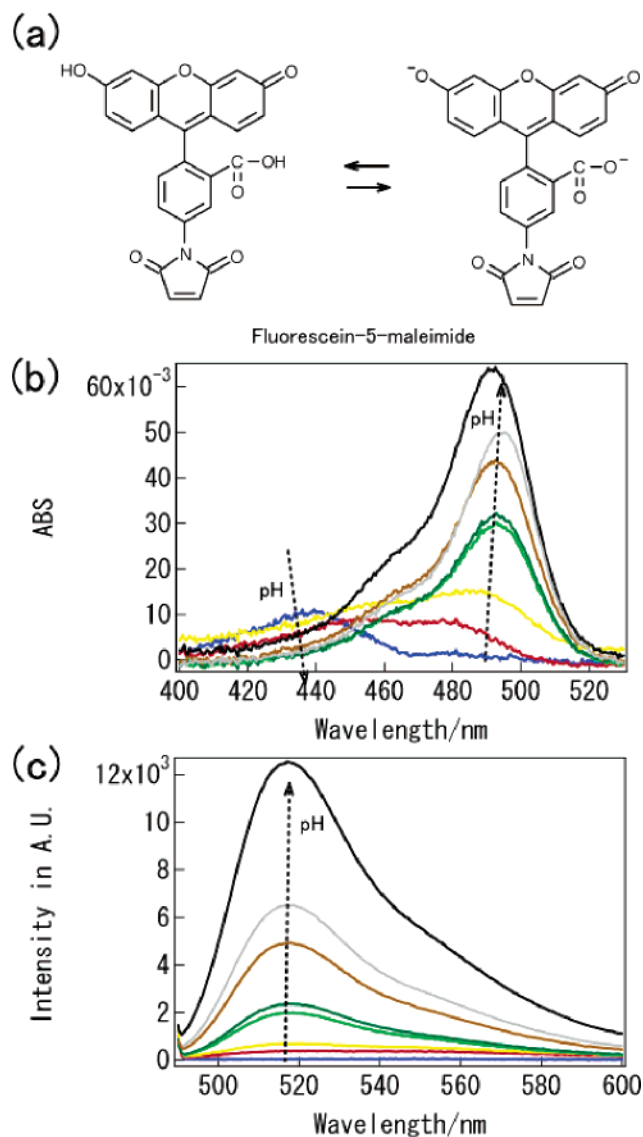
Figure 2. Properties of the fluorescent probe (a). Chemical structures of FLU (b). (c) Absorption and fluorescence spectra of FLU molecules at various pH. The blue, red, yellow, light green, dark green, brown, gray, and black line represent the spectra obtained at pH 2.4, 4.6, 6.0, 7.6, 8.2, 8.6, 9.2, and 10.3, respectively. The wavelength of the excitation light in panel c is 488 nm.

of an inverted CLSM (Nanofinder, Tokyo Instruments, Tokyo, Japan) and an AFM (Smena liquid head, NT$-$MDT, Moscow, Russia) inserted in the open space above the CLSM. The excitation light source is an Ar$^+$ laser (488 nm, Nippon Laser, Japan). The optical spectra of the samples are measured with a
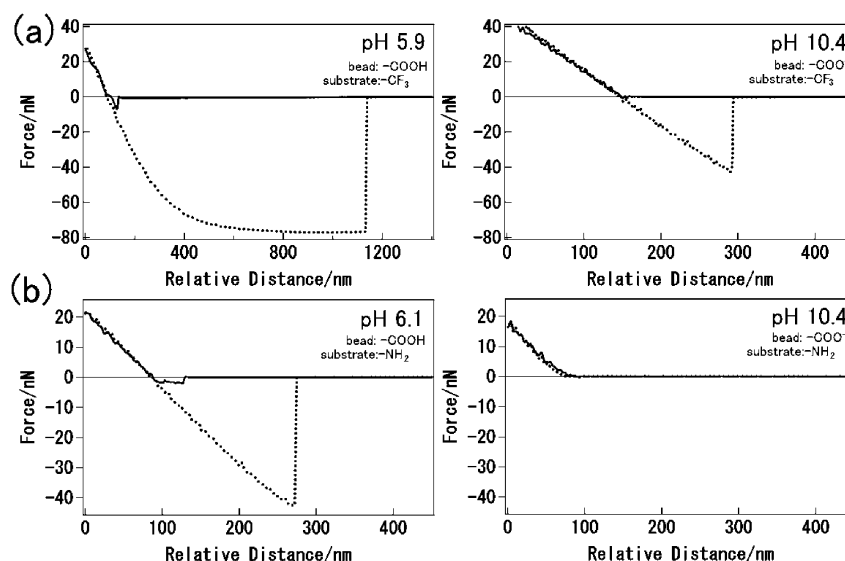
Figure 3. Typical force distance curve when the AFM probe to which a polystyrene microbead was attached was brought into contact with the modified glass surface in a liquid. The vertical and horizontal axes represent the applied force and the relative displacement of the piezo element, respectively. The solid and dotted lines represent the approach and the retract curves, respectively. The velocity of the AFM probe was adjusted to 2 μm/s. (a) The force distance curves obtained when the AFM probe was brought into contact with the $-CF_3$ terminated surface at pH 5.9 and 10.4. (b) The force distance curves obtained when the AFM probe was brought into contact with the $-NH_2$ terminated surface at pH 6.1 and 10.4.

cooled CCD camera (Andor Technology, Belfast, Northern Ireland) equipped with a spectrograph ($f = 56$ cm, 200 grooves/mm grating). This CLSM is equipped with a pin hole (60 μm diameter) for improving the spatial resolution. The AFM status information during the force curve measurement can be collected, and the optical spectrum can be synchronously measured by using a CLSM/AFM controller built by us. All of the experiments were performed according to the following procedure: [30] The AFM probe was brought into contact with the substrate surface, and the substrate was fixed. The measurement point of the CLSM was fixed after adjusting it to correspond with the contact area of the AFM probe. A force curve measurement was performed by the AFM. Only the AFM probe was moved vertically above the substrate surface. Spectroscopic measurements were performed at arbitrary AFM probe positions, maintaining the exposure time and input power of the excitation light source constant. We recorded the vertical positions of the AFM probe at which the spectra were measured and plotted them in the obtained force−distance curve.

2.3. Experimental Conditions. In all of the experiments, the input power of the excitation light was adjusted to 5 μW. The exposure time of CCD was adjusted to 1 s. The pH of the liquid phase was varied from 3 to 11 using buffer solutions. We used citrate buffered saline, phosphate buffered saline, and carbonate buffered saline appropriately. The ionic strength was kept constant in all the experiments by adjusting the concentration of the buffer solution to 100 mM.

3. Results and Discussion

In this study, two experimental approaches were used to measure the surface force between a carboxylated polystyrene microbead and a substrate surface. First, the surface force was measured by the traditional AFM measurement; measurements were made in a liquid at various pH, titration curves were obtained, and the relation between the surface force and the functional group on the surfaces was discussed. Next, the surface force measurements were carried out with the simultaneous
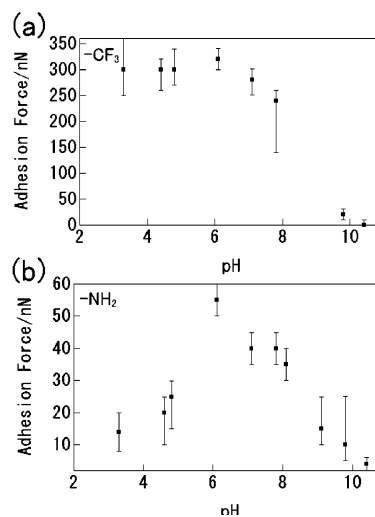
detection of the solvent molecules in the contact area by the force curve mode CLSM/AFM. Finally, the two methods were compared.

First, we performed the adhesion force measurement without the modification of the microbead surface with FLU molecules. Therefore, the surface of the AFM probe had both a polystyrene surface and $-COOH$ groups. The cover glass modified with APDS has a hydrophilic surface because of the terminal functional groups $-NH_2$. The cover glass modified with FPDS has the functional groups $-CF_3$; therefore, its surface is hydrophobic. Both surfaces have elastic properties similar to that of the unmodified glass surface because the thickness of each modification layer is small. The representative data of the force distance curve are shown in Figure 3. The adhesion forces between the AFM probe and sample surface are observed in the retract phase of each curve. It is clearly seen that the adhesion force measured at pH 5.9 was larger than that measured at pH 10.44 when the AFM probe was brought into contact with the $-CF_3$ surface. In contrast, when the AFM probe was brought into contact with the $-NH_2$ surface, the adhesion force measured at pH 6.1 was larger than that measured at pH 10.4. Further, the adhesion force on the $-CF_3$ surface was larger than that on the $-NH_2$ surface. The variation in the observed adhesion forces was because of fluctuation of the contact area between the microbead and substrate surface. Therefore, we performed the adhesion force measurements several times in order to obtain the static value and repeated these measurements at various pH levels to investigate the phenomenon in detail. The titration curve is shown in Figure 4. On the $-CF_3$ surface, the adhesion force varied dramatically around pH 7, and a strong adhesion force of 200−300 nN was observed below this pH. However, the adhesion force was diminished above this pH; it was approximately 20 nN. It is considered that the decrease and elimination of the adhesion force are consistent with the deprotonation of the carboxyl groups on the bead surface because the $-CF_3$ surface did not have protonated groups. As described above, the pK_a of the protonated groups bound to the surface is remarkably different from the bulk value. In addition,

Direct Detection of the Solvent Molecules

J. Phys. Chem. C, Vol. 111, No. 19, 2007 **7101**
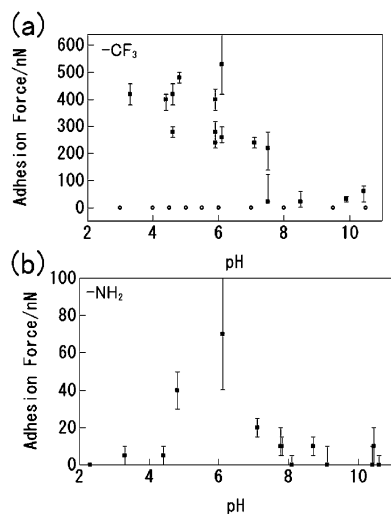
Figure 4. Titration curve of the adhesion forces observed between an unmodified carboxylated polystyrene microbead and the modified substrate surfaces. All of the averaged adhesion force values were determined from the histogram of the adhesion values obtained from at least 50 individual force distance curves, and the error bar was added to each value. The vertical and horizontal axes correspond to the averaged adhesion force and pH, respectively. (a) The average adhesion values obtained when the AFM probe was brought into contact with the $-CF_3$ terminated surface and the unmodified glass surface at various pH. The solid squares and the open circles represent the adhesion values observed on the $-CF_3$ terminated surface and unmodified glass surface, respectively. (b) The average adhesion values obtained when the AFM probe was brought into contact with the $-NH_2$ surface at various pH. The solid squares represent the adhesion values observed on the $-NH_2$ surface.


Figure 5. Titration curve of the adhesion forces observed between a carboxylated polystyrene microbead and modified substrate surfaces when FLU molecules were introduced onto the surface of the carboxylated microbead. All of the averaged adhesion force values were determined from the histogram of the adhesion values obtained from at least 50 individual force distance curves, and the error bar was added to each value. The vertical and horizontal axes correspond to the averaged adhesion force and the pH, respectively. (a) The averaged adhesion values obtained when the AFM probe was brought into contact with the $-CF_3$ terminated surface at various pH. The solid squares represent the adhesion values observed with the $-CF_3$ terminated surface. (b) The averaged adhesion values obtained when the AFM probe was brought into contact with the $-NH_2$ terminated surface at various pH. The solid squares represent the adhesion values observed on the $-NH_2$ terminated surface.

it has been reported that the pK_a of $-COOH$ groups on the surface is approximately $2-3$ pK_a units higher than the bulk value.[16] In the present experiments, the pK_a was approximately 7, which is slightly higher than the reported value. It is considered that the presence of a low dielectric permittivity region surrounding the acidic or basic groups affects the pK_a shift. The material of a microbead is polystyrene, which is hydrophobic. The $-CF_3$ surface is also hydrophobic, and hydrogen bonding or electrostatic interaction might not occur. Therefore, the observed large adhesion force at low pH originates from the hydrophobic interaction between the $-CF_3$ surface and bead surface. Hydrophobic interactions generally act between hydrophobic surfaces in aqueous solution. The bead surface has the hydrophilic $-COOH$ groups and the hydrophobic polystyrene surface. It is assumed that (1) the density of the $-COOH$ group is not high enough to make the surface hydrophilic or (2) the surface has a surface roughness and the polystyrene surface may be exposed. Further, it is considered that the deprotonated carboxyl group ($-COO^-$) is more hydrophilic than the protonated form ($-COOH$) because it is ionized. Thus, the ionized carboxyl groups ($-COO^-$) diminish the adhesion force. Figure 4b shows the titration curve obtained when the AFM probe was brought into contact with the $-NH_2$ surface. The observed adhesion force value was approximately one-fifth that on the $-CF_3$ surface. In addition, the adhesion force dramatically varied at around pH 4.5 and pH 7. It is considered that the adhesion force above pH 7 decreased because of the ionization of the $-COOH$ groups on the bead surface. Further, it is considered that the decrease in the adhesion force below pH 4.5 is consistent with the ionization of the amino groups ($-NH_3^+$) on the substrate surface. It has been reported that the pK_a of the $-NH_2$ groups on the surface is significantly lower than the bulk value. The obtained pK_a of 4.5 is similar to

the reported value.[16] When the pH was below 4.5, most of the amino groups were ionized ($-NH_3^+$) and most of the carboxyl groups on the bead surface were protonated ($-COOH$); when between 4.5 and 7, most of the amino groups were in their neutral form ($-NH_2$) and most of the carboxyl groups were also protonated ($-COOH$); and when above 7, most amino groups were in their neutral form ($-NH_2$) and most of the carboxyl groups were ionized ($-COO^-$). Therefore, because (1) both the amino and carboxyl groups were not ionized, (2) the substrate surface was hydrophilic, and (3) the observed adhesion force was smaller than that when it was brought into contact with the $-CF_3$ surface, the adhesion force observed between the pH of 4.5 and 7 originates from a hydrogen bonding force between the neutral $-NH_2$ and $-COOH$ groups. In contrast, the hydrogen bonding force diminished below pH 4.5 and above pH 7.0 because either the amino or carboxyl groups were ionized. Moreover, when the AFM probe was brought into contact with an unmodified glass surface, no adhesion was observed (see Figure 4a). The bead surface did not adhere to the glass surface because the glass surface had a negative charge in the experimental condition.

Next, we performed the same pH-dependence measurement for the adhesion force when FLU was attached to the bead surface. The obtained titration curve is shown in Figure 5. As compared to the data obtained with the unmodified microbead (see Figure 4), the adhesion force is observed to decrease slightly in both cases. Further, it is clearly seen that the pK_a of the $-COOH$ groups on the bead surface shifted slightly to the alkaline side and that the change in the adhesion force is gradual. It is considered as follows: the $-COOH$ groups on the bead surface were used for the introduction of FLU molecules to the surface. However, cysteine molecules also possess $-COOH$ groups, and FLU has both a $-COOH$ group and an ionizable
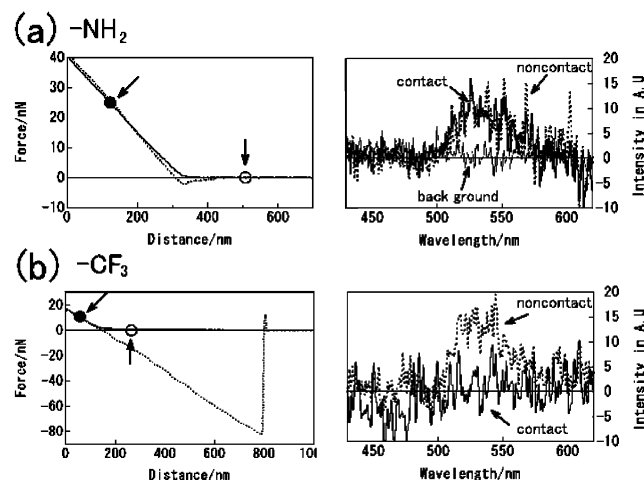
Figure 6. Force−distance curves and fluorescence spectra of the contact area. Panels a and b show the results for the −NH₂ and −CF₃ terminated surfaces, respectively. The spectra shown by solid and dotted lines were taken at the distances shown by solid and open circles in the force−distance curve, respectively. The baselines of these spectra were defined as the noise including the dark current of the detector and stray light from outside the experimental system. The background level (such as fluorescence of the unmodified bead etc.) is indicated by the thin line in Figure 6a.

aromatic −OH group. Thus, the density of the ionizable groups on the bead surface increased, and this might have shifted the pK_a to the alkaline side. In addition, the pK_a of the aromatic −OH groups in FLU is slightly higher than that of the −COOH groups. Thus, the properties of both the −COOH and aromatic −OH groups were simultaneously observed in the curve.

In summary, the AFM measurement revealed that the hydrophobic interaction operates when the carboxylated polystyrene microbead is brought into contact with the −CF₃ surface, and the hydrogen bonding force, when the microbead is in contact with the −NH₂ surface. Next, the adhesion force measurement was carried out with the simultaneous detection of solvent molecules by the force curve mode CLSM/AFM.

We measured the change in the fluorescence spectra of the fluorophore that was attached to the bead surface and simultaneously measured the adhesion force between the bead and the sample surface in an aqueous solution (pH 9.5, 100 mM carbonate buffered saline).[29] The reason why the measurements were performed at pH 9.5 is that most fluorescein molecules become the H⁺-dissociated form at the aqueous condition. The representative data are shown in Figure 6. The solid lines in Figure 6, panels a and b, show the fluorescence spectra of the contact area; these spectra were obtained when the AFM probe was in contact with the substrate surfaces that had terminal groups −NH₂ and −CF₃, respectively. The vertical positions of the AFM are indicated by solid circles in the figure. The dotted line shows the fluorescence spectrum obtained when the probe was in the noncontact condition. Here, the positions of the AFM probe are indicated by open circles. A large adhesion force was observed when the AFM probe was brought into contact with the −CF₃ surface. However, no adhesion force was observed when it was brought into contact with the −NH₂ surface. These results show that the FLU in the contact area was not quenched by the −NH₂ surface but by the −CF₃ surface. Background light such as fluorescence from the unmodified bead or the modified glass surface was not observed in these experimental conditions (see Figure 6a; thin line). Furthermore, no change in the fluorescence intensity was observed when the
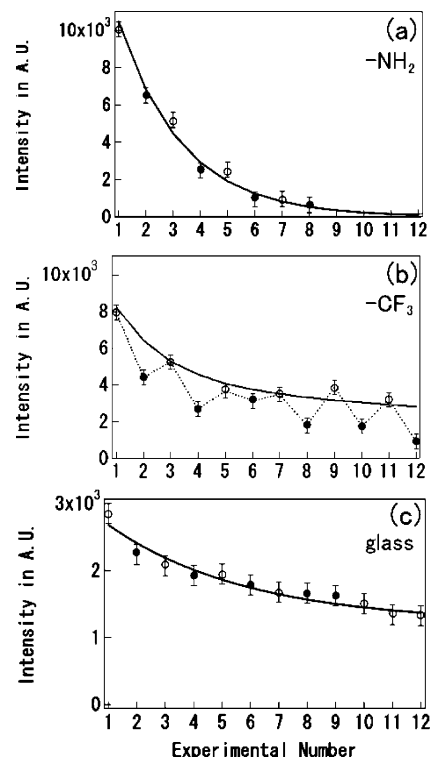
Figure 7. Integrated fluorescence intensity of fluorescein (500−600 nm) on the surface of an AFM probe. Panels a−c show the typical results for the measurements on the −NH₂ terminated surfaces, −CF₃ terminated surfaces, and glass surfaces, respectively. In this figure, solid and open circles represent the data obtained when the AFM probe was in contact with the surface by applying a load of 5 nN and when the probe was separated from the surface (within approximately 200 nm), respectively. The solid line is the photobleaching curve created on the basis of an open circle. In addition, the broken line in panel b shows the temporal change in the fluorescence intensity. The error bars were statistically calculated by integrating (500−600 nm) the data measured with only the background noise.

probe was in contact with an unmodified surface. The fluorescence intensity ordinarily decreased because of the photobleaching of the fluorescent dye. In addition, the observed fluorescence changes fluctuated because of the fluctuation of the contact area between the microbead and the substrate surface. Therefore, in order to discuss this issue qualitatively and quantitatively, the fluorescence spectra of the contact area were measured with the application of a fixed load of approximately 5 nN, and same measurements were performed by alternately repeating contact and noncontact (within approximately 200 nm above the substrate) conditions.[30] The integrated fluorescence intensity in the 500−600 nm region is summarized in Figure 7. Figure 7a−c shows the typical results for the measurements of the −NH₂ surfaces, −CF₃ surfaces, and unmodified glass surfaces, respectively. In this figure, the vertical axis shows the integrated fluorescence intensity and the horizontal axis corresponds to the sequential numbering of the spectroscopic measurements starting from 1 (exposure time 1 s, input power of excitation light 5 μW). In Figure 7, solid and open circles represent the data obtained when the AFM probe was in the contact and noncontact conditions, respectively. The measured fluorescence intensity decreased in both cases because of the photobleaching of the dyes. These photobleaching curves exhibited different temporal profiles from one another. The difference between the two photobleaching curves in Figure 7 is not due to the background noise or difference in the modified surface but due to the difference in the effect of oxygen on the degradation of

Direct Detection of the Solvent Molecules

J. Phys. Chem. C, Vol. 111, No. 19, 2007 **7103**

the dyes. Thus, we alternately measured the fluorescence intensity in the contact and noncontact conditions and considered the difference between them. Although the fluorescence intensity is not significantly different in either the contact or noncontact conditions for the $-NH_2$ surfaces and the unmodified glass surface, Figure 7b shows that for the $-CF_3$ surfaces the fluorescence intensity in the contact condition was remarkably weaker than that in noncontact. As a result, it can be confirmed that the quenching of the fluorescence is not due to the photobleaching but the contact of the probe with the hydrophobic surface. The fluorescence spectra in Figure 6 were measured when the fluorescence of the dye molecules was stable against the photobleaching; thus, Figure 6 represents an example of the perfect quenching of the fluorescence. However, the efficiency of this quenching always fluctuated. If the substrate surface has a high compliance, the contact area should increase with the compression force.[38] However, since both the polystyrene microbeads and the glass substrates are fairly hard, it is considered that the contact area between the microbead and the glass surfaces is smaller than the region monitored by the CLSM. Therefore, the fluorescence from the dyes in bulk was also measured in a manner similar to that of our previous experimental results.[29−32]

The diameter of the microbead is 10 μm, and the substrate surface is a monolayer. Actually, the surface roughness of the substrate surface was observed with the atomic force microscope. It was <1 nm. On the other hand, although it is hard to estimate the density of the carboxyl groups and the roughness on the microbead, our group previously observed the surface of the microbead with a scanning electron microscope.[33] As a result, the microbead could be observed as a sphere and the remarkable roughness structure, such as a projection or a hole, was not observed. Furthermore, it has been reported that the adhesion force affects other parameters, such as the solvent viscosity, when the material is soft like a biopolymer.[39] However, the force−distance curves in Figure 3 show that the compression or the extension of the materials could not be observed. Therefore, we assumed that the material is quite hard, the surface roughness was negligible, and the microbead was approximated to a sphere. The adhesion force was theoretically estimated using JKR theory, which is given by the following:[1]

$$F_{ad} = 1.5\pi R W_{132} \tag{1}$$

where R is the radius of a tip and W_{132} is work of adhesion between solid surface 1 and solid surface 2 in medium 3. The JKR theory considers that only short-range interfacial forces are operative and that a finite contact area exists upon rupture. The contact area of an AFM probe was defined in JKR theory as follows:

$$a = \left(\frac{1.5\pi R^2 W_{132}}{K}\right)^{1/3} \tag{2}$$

where a is the radius of the contact area and K is the effective elastic modulus of the microcontact, which is given by the following:

$$\frac{1}{K} = \frac{3}{4}\left[\left(\frac{(1-\nu_1^2)}{E_1}\right) + \left(\frac{(1-\nu_2^2)}{E_2}\right)\right] \tag{3}$$

where E is the Young's modulus and ν is the Poisson ratio of the tip and sample material.

Therefore, the theoretical contact area can be estimated from the observed adhesion force with the following equation:

$$a = \left(\frac{RF_{ad}}{K}\right)^{1/3} \tag{4}$$

where the radius of the contact area is denoted by a. Thus, the contact area is equal to πa^2. Thus, it is directly proportional to the two-third power of the adhesion force. It should be noted that the titration curves in Figure 5 indicate that the averaged adhesion force on the $-CF_3$ surfaces is approximately twice as large as that on the $-NH_2$ surfaces at pH 9.5. Therefore, the contact area between the bead surface and the $-CF_3$ surface is $2^{2/3} = 1.5874$ times larger than that between the bead and the $-NH_2$ surface. However, similar experiments were repeated, and the ratio of the intensity of the contact spectra to that of the noncontact spectra was statistically calculated to be 70% ($\pm$20). If the FLU molecules in contact area were perfectly quenched, the fluorescence quenching ratio shows the ratio of the contact area to the area of the measurement region. If they were also quenched when in contact with the $-NH_2$ surface, it is considered that we could detect the fluorescence change because the difference in the contact areas was small. Therefore, the fluorescence change observed when in contact with the $-CF_3$ surface is not due to the difference in the contact areas between them.

The previous titration measurement revealed that the observed adhesion force between the microbead and the $-CF_3$ surface originated from the hydrophobic interaction. Further, it has been determined that the hydrogen bonding force operates when the AFM probe is in contact with the $-NH_2$ surface. On the basis of these results, we consider the following (see Figure 7): The microbead has both the hydrophobic polystyrene surface and the hydrophilic surface that has ionized groups. When the hydrophobic interaction operates between solid surfaces, the solvent molecules between them are removed, and the surfaces strongly adhere to each other. Although the groups in the H^+-dissociated form are generally more stable than those in the H^+-undissociated form at pH 9.5, the charged groups are compulsorily altered to their neutral forms in the contact area because they are unstable in the hydrophobic condition. FLU is more fluorescent in the H^+-dissociated form than in the H^+-undissociated form. Therefore, the FLU molecules in the contact condition were quenched. However, on the $-NH_2$ surface, the adhesion originates from hydrogen bonding, which is an interaction between hydrophilic surfaces. Therefore, the fluorescence intensity was not changed when the AFM probe was brought into contact with the surface.

These experimental results are in good agreement with the classical theory. It indicates that the force curve mode CLSM/AFM measurement enables us to detect the solvent molecules in the contact area and conduct simultaneous force measurements. Although only the applied force and the relative distance of an AFM probe can generally be acquired by the conventional AFM system, the spectroscopic data can be provided as additional information along with the standard AFM measurement data using this technique. This implies that the observed adhesion force can be identified separately.

4. Conclusion

In this study, we attempted to observe the water molecules in the contact area using the force curve mode CLSM/AFM technique. As the results, the detection of the water molecules in the contact was successful. When the hydrophobic interaction

operates, the solvent molecules are removed and the hydrophobic surfaces stabilize each other by making the contact area hydrophobic. However, when the hydrophilic interaction such as hydrogen bonding operates, the solvent molecules exist in the contact area. To the best of our knowledge, nobody has reported such experimental results obtained by the direct observation of the solvent property and by the simultaneous measurement of the adhesion force using an AFM system.

In the future, it is expected that more valuable information will be obtained from the proposed simultaneous measurement by using different types of sensitive dyes having fluorescence wavelengths dependent on the permittivity of the solvent around them. Furthermore, more quantitative data will be able to be obtained by the improvement of the spatial resolution of the integrated system.

References and Notes

(1) Israelachvili, J. N. *Intermolecular and Surface Forces*, 2nd ed.; Academic Press: London, 1992.

(2) Ducker, W. A.; Senden, T. J.; Pashley, R. M. *Langmuir* **1992**, *8*, 1831.

(3) Lin, X. Y.; Crenzet, F.; Arribart, H. *J. Phys. Chem.* **1993**, *97*, 7272.

(4) Hillier, A. C.; Kim, S.; Bard, A. J. *J. Phys. Chem.* **1996**, *100*, 18808.

(5) Takano, H.; Kenseth, J. R.; Wong, S.-S.; O'Brien, J. C.; Porter, M. D. *Chem. Rev.* **1999**, *99*, 2845.

(6) Israelachvili, J. N.; Pashley, R. M. *Nature* **1982**, *300*, 341.

(7) Butt, H.-J. *Biophys. J.* **1991**, *60*, 1438.

(8) Frisbie, C. D.; Rozsnyai, L. F.; Noy, A.; Wringhton, M. S.; Lieber, C. M. *Science* **1994**, *265*, 2071.

(9) Noy, A.; Frisbie, C. D.; Rozsnyai, L. F.; Wrighton, M. S.; Lieber, C. M. *J. Am. Chem. Soc.* **1995**, *117*, 7943.

(10) Van der Werf, K. O.; Putman, C. A. J.; de Grooth, B. G.; Greve, J. *Appl. Phys. Lett.* **1994**, *65*, 1195.

(11) Miyatani, T.; Horii, M.; Rosa, A.; Fujihira, M. *Appl. Phys. Lett.* **1997**, *71*, 2632.

(12) Noy, A.; Sanders, C. H.; Vezenov, D. V.; Wong, S. S.; Lieber, C. M. *Langmuir* **1998**, *14*, 1508.

(13) Schneider, M.; Zhu, M.; Papastavrou, G.; Akari, S.; Möhwald, H. *Langmuir* **2002**, *18*, 602.

(14) He, H. X.; Li, C. Z.; Song, J. Q.; Mu, T.; Wang, L.; Zhang, H. L.; Liu, Z. F. *Mol. Cryst. Liq. Cryst.* **1997**, *294*, 99.

(15) He, H. X.; Li, C. Z.; Wang, J. M.; Xu, X. J.; Liu, Z. F. *Acta. Phys. Chim. Sin.* **1997**, *13*, 293.

(16) Vezenov, D. V.; Noy, A.; Rozsnyai, L. F.; Lieber, C. M. *J. Am. Chem. Soc.* **1997**, *119*, 2006.

(17) Van der Vegte, E. W.; Hadziioannou, G. *J. Phys. Chem. B* **1997**, *101*, 9563.

(18) Van der Vegte, E. W.; Hadziioannou, G. *Langmuir* **1997**, *13*, 4357.

(19) Zhang, H.; He, H.-X.; Mu, T.; Liu, Z.- F. *Thin. Solid. Films.* **1998**, *327-329*, 778.

(20) Weisenhorn, A. L.; Maivaid, P.; Butt, H.-J.; Hansma, P. K. *Phys. Rev. B* **1992**, *45*, 11226.

(21) Thomas, R. C.; Houston, J. E.; Crooks, R. M.; Kim, T.; Michalske, T. A. *J. Am. Chem. Soc.* **1995**, *117*, 3830.

(22) Sato, F.; Okui, H.; Akiba, U.; Suga, K.; Fujihira, M. *Ultramicroscopy* **2003**, *97*, 303.

(23) Tsukruk, V. V.; Bliznyuk, V. N. *Langmuir* **1998**, *14*, 446.

(24) Sinniah, S. K.; Steel, A. B.; Miller, C. J.; Reutt-Robey, J. E. *J. Am. Chem. Soc.* **1996**, *118*, 8925.

(25) Bain, C. D.; Whitesides, G. M. *Langmuir* **1989**, *5*, 1370.

(26) Balachander, N.; Sukenik, C. N. *Langmuir* **1990**, *6*, 1621.

(27) Creager, S. E.; Clarke, J. *Langmuir* **1994**, *10*, 3675.

(28) Lee, T. R.; Carey, R. I.; Biebuyck, H. A.; Whitesides, G. M. *Langmuir* **1994**, *10*, 741.

(29) Kodama, T.; Ohtani, H.; Arakawa, H.; Ikai, A. *Chem. Phys. Lett.* **2004**, *385*, 507.

(30) Kodama, T.; Ohtani, H.; Arakawa, H.; Ikai, A. *Jpn. J. Appl. Phys.* **2004**, *43*, 4580.

(31) Kodama, T.; Ohtani, H.; Arakawa, H.; Ikai, A. *Appl. Phys. Lett.* **2005**, *86*, 043901.

(32) Kodama, T.; Ohtani, H.; Arakawa, H.; Ikai, A. *Ultramicroscopy* **2005**, *105*, 189.

(33) Hyonchol, K.; Arakawa, H.; Osada, T.; Ikai, A. *Colloids Surf. B* **2002**, *25*, 33.

(34) Ducker, W. A.; Senden, T. J.; Pashley, R. M. *Nature* **1991**, *353*, 239.

(35) Karaman, M. E.; Meagher, L.; Pashley, R. M. *Langmuir* **1993**, *9*, 1220.

(36) Waddell, T. G.; Leyden, D. E.; DeBello, M. T. *J. Am. Chem. Soc.* **1981**, *103*, 5303.

(37) Ulman, A. *Chem. Rev.* **1996**, *96*, 1533.

(38) Weihs, T. P.; Nawaz, Z.; Jarvis, S. P.; Pethica, J. B. *Appl. Phys. Lett.* **1991**, *59*, 3536.

(39) Abu-Lail, N. I.; Camesano, T. A. *Biomacromolecules* **2003**, *4*, 1000.